Composite Structures 295 (2022) 115847

Contents lists available at ScienceDirect

Composite Structures

journal homepage: www.elsevier.com/locate/compstruct

# Thermally induced mechanical work and warpage compensation of asymmetric laminates

Bruno Vermes, Tibor Czigany *

*Department of Polymer Engineering, Faculty of Mechanical Engineering, Budapest University of Technology and Economics, Műegyetem rkp. 3., H-1111 Budapest, Hungary*
*MTA-BME Research Group for Composite Science and Technology, Műegyetem rkp. 3., H-1111 Budapest, Hungary*

ARTICLE INFO

*Keywords:*
Thermally induced work
Warpage compensation
Monostability and bistability
Tooling

ABSTRACT

The thermal warpage of asymmetric laminates can be converted into mechanical work. However, thermal warpage is usually unwanted, and can be mitigated with compensatory tool designs. This paper investigates both concepts, focusing on monostability, bistability and the transitional behaviour between the two. Numerical and experimental results showed that the maximum achievable mechanical work goes through a local maximum and then a local minimum as the laminate transitions from bistability to monostability with a decreasing edge length to thickness ratio. The local maximum was correlated with the appearance of the second principal curvature, while the local minimum took place just before reaching the bifurcation point. We successfully manufactured laminates from the monostable region flat using tools with two significant principal curvatures. Laminates from the bistable region were successfully transformed to monostable laminates with similar tools, implying that successful warpage compensation of bistable laminates requires tools that include both principal curvatures.

## 1. Introduction

Composites in the industry are mainly used for their outstanding specific mechanical properties (i.e. strength and stiffness); however, many publications have shown that they can be given extra features making them even more valuable. Additional features can be anything from self-healing [1,2] or self-monitoring [3,4] to pseudo-ductility [5–7] or morphing behaviour [8,9]. Morphing behaviour is the result of a direct, intrinsic relationship between loads and deformations of different modes and is one of the most fundamental additional features of composites. This is how helicopter rotor blades can twist under centrifugal tensile loads [10,11], or turbine blades can twist under aerodynamic or hydrodynamic bending loads [12–14] for improved working efficiency. Since the constituting plies have different thermal expansion in different directions, the morphing of laminates can be induced thermally, too. Depending on various parameters (e.g. material properties, layup and edge length to thickness ratio), asymmetric laminates may have two distinct stable shapes instead of one. Hyer [15,16] was the first to publish some of the fundamental characteristics of bistable laminates. Bistable laminates have cylindrical shapes instead of saddle shapes predicted by the Classical Lamination Theory (CLT). One of the principal curvatures in either stable shape is virtually zero (except close the bifurcation point, which separates the monostable region from the bistable region), and the stable shapes can reversibly transform into each other via a snap-through effect. The first and second principal curvatures of a surface are the largest curvature and the curvature perpendicular to the largest curvature at a given point (usually defined at the mid-point of laminates). Since their first appearance in the scientific literature, bistable laminates have been extensively researched [17,18]. There are ways to achieve bistability other than optimising layups (e.g. prestressed laminates [19,20] and morphing structures [21,22]); however, this paper focuses on layup-driven morphing. Tawfik *et al.* [23] numerically and experimentally demonstrated how the critical load necessary for the snap-through effect to take place depends on the edge length to thickness ratio of a cross-ply bistable laminate, while others built models to predict the magnitude of the critical snap-through load or the geometry of the stable shapes [24,25]. The effects of moisture [26], polymer composite and metal hybrids [27,28] or piezoelectric actuation [29,30] are some of the various other aspects of bistable laminates that have already been investigated. However, the thermally induced mechanical work of asymmetric laminates is still an area that needs further investigation, especially near the transition between the bistable and monostable states. The physical meaning of thermally induced mechanical work is how much mechanical work can be

* Corresponding author.
*E-mail addresses:* czigany@pt.bme.hu, czigany@eik.bme.hu (T. Czigany).

https://doi.org/10.1016/j.compstruct.2022.115847
Received 21 June 2021; Received in revised form 29 April 2022; Accepted 25 May 2022
Available online 28 May 2022

harvested at a given location of the asymmetric laminate due to its thermal warpage.

Layup asymmetry can be an advantage when exploiting the thermally induced morphing of laminates. However, manufacturing-induced warpage is usually unwanted and therefore should be mitigated. Some warpage mitigation methods have already been proven to be effective for asymmetric laminates. Layup homogenisation repeats the same asymmetric sub-laminates on top of each other until the whole laminate is practically warp-free [31,32]. Also, there are asymmetric laminates that are hygro-thermally curvature-stable, but they are rare [33,34]. These methods make the shape of the laminates practically independent of the temperature as if the layup was symmetric. But a temperature-dependent shape is a requirement in the case of composites with thermally induced morphing capabilities. Compensating for manufacturing-induced warpage by modifying the shape of the tools is not a new idea [35–39]; however, manufacturing asymmetric laminates - especially bistable ones - flat is still a challenge. Even asymmetric laminates are warp-free at the curing temperature, and they only warp when cooled down. With curved tools, the warp-free geometry of the laminate is modified so that the laminate can warp to the desired geometry when cooled down. This method does not mitigate warpage on the material level but compensates for it.

The aim of this paper is twofold. First, we investigate the thermally induced mechanical work of an asymmetric layup (due to morphing with changing temperatures) and discuss how the bistable-monostable transition affects the maximum achievable work. The example layup is the result of a full-field analytical search for maximum thermal warpage. Finally, we investigate how a tool compensation method can be applied to monostable and bistable laminates in order to manufacture laminates that are flat at room temperature but can demonstrate thermally induced morphing with changing temperatures. Both the warpage and the thermally induced work depend greatly on factors such as the material properties and layup structure of the laminate as well as the temperature; therefore, all determining factors are discussed in the following sections to make the results reproducible.

## 2. Full-field search for the most significantly warping layup based on the CLT

In this section, we aim to find an example layup that is suitable for both the thermally induced mechanical work and the warpage mitigation investigations. Such a layup needs to display considerable thermal warpage. The search requires the examination of a large number of layup permutations, where an analytical approach is the most effective and the CLT is a well-established analytical method to calculate the constitutive equations for thin laminates in the elastic range. The CLT reaches its limitations in terms of accuracy when it comes to large out of plane deformations, and it predicts the warped shape to be a saddle even in the case of laminates that are bistable in reality. However, the quantitative results of the analytical calculations are not the primary focus here. The idea is to find the laminate with the largest thermal warpage based on the CLT and then use that layup for the investigations. The most significantly warping laminate based on the CLT is expected to be amongst the most significantly warping laminates in reality, which is the main point of the analytical search. Since our laminate is loaded thermally rather than mechanically, the load definition of the CLT needed some adjustment [40].

### 2.1. Calculation of the thermal deformation

According to the CLT, loads can be calculated from the ABD matrix (*[ABD]*) - specific to any layup - and the strains. Conversely, strains can be calculated from the inverse ABD matrix (*[ABD]'*) and the loads. This relation stands for thermal loads, too (1).

$$\begin{Bmatrix} \varepsilon_x^0 \\ \varepsilon_y^0 \\ \varepsilon_{xy}^0 \\ \kappa_x \\ \kappa_y \\ \kappa_{xy} \end{Bmatrix} = \begin{bmatrix} [A][B] \\ [B][D] \end{bmatrix}' \begin{Bmatrix} N_x^T \\ N_y^T \\ N_{xy}^T \\ M_x^T \\ M_y^T \\ M_{xy}^T \end{Bmatrix} \tag{1}$$

where $\varepsilon_x^0, \varepsilon_y^0$ and $\varepsilon_{xy}^0$ are the mid-plane strains, $\kappa_x, \kappa_y$ and $\kappa_{xy}$ are the curvatures, while $N_x^T, N_y^T$ and $N_{xy}^T$ are the thermal forces per unit length and $M_x^T, M_y^T$ and $M_{xy}^T$ are the thermal moments per unit length.

The difference between mechanical and thermal CLT is the definition of the loads [40]. For a thermally loaded laminate, the loads greatly depend on the layup. This is because of the directionality of the thermal expansion. Each layup is loaded differently, even if they experience the same change in temperature (2,3).

$$\begin{Bmatrix} N_x^T \\ N_y^T \\ N_{xy}^T \end{Bmatrix} = \Delta T \sum_{k=1}^{N} [\overline{Q}]^k \begin{Bmatrix} \alpha_x \\ \alpha_y \\ \alpha_{xy} \end{Bmatrix}^k t_k \tag{2}$$

$$\begin{Bmatrix} M_x^T \\ M_y^T \\ M_{xy}^T \end{Bmatrix} = -\Delta T \sum_{k=1}^{N} [\overline{Q}]^k \begin{Bmatrix} \alpha_x \\ \alpha_y \\ \alpha_{xy} \end{Bmatrix}^k t_k \overline{z}_k \tag{3}$$

where $\Delta T$ is the change in temperature ($^\circ C$), $k$ is the ordinal number of the ply in the layup, $[\overline{Q}]$ is the stiffness matrix of the ply in the structural direction $\alpha_x, \alpha_x$ and $\alpha_{xy}$ are the in-plane thermal coefficients of the ply in the structural direction (there are only two in the material direction), $t_k$ is the thickness of the ply and $\overline{z}_k$ is the distance of the ply mid-plane from the laminate mid-plane. The warpage of the thermally loaded laminate can then be defined from the curvatures ($\kappa_x, \kappa_y$ and $\kappa_{xy}$). A simple way to quantify warpage is by calculating the height of the encasing cuboid of the laminate (Fig. 1). A larger height means more significant warpage.

### 2.2. Layup search with a MATLAB algorithm

For the calculations, simulations and experiments, we worked with Hexcel's IM7/913 carbon-epoxy UD prepreg. Table 1 contains the relevant material data.

where $E_1$, $E_2$ and $G_{12}$ are the in-plane moduli, $\upsilon_{12}$ is the Poisson's ratio, $t_{ply}$ is the cured ply thickness and $\alpha_0$ and $\alpha_{90}$ are the coefficients of thermal expansion in the fibre direction and in the transverse direction.

Other than the data in Table 1, there are two essential inputs for the calculations: the layup and the temperature change.

To allow for a full-field search, we analysed 4-ply laminates with a 15° orientation increment (increment by which ply orientations can be rotated). With more than 20,000 possible layup permutations (permutation with repetition), this provided a good range of mechanical behaviour to find a layup with a large out-of-plane deformation when heated or cooled. At the same time, the computational effort needed for the calculations was still manageable for a desktop PC. We developed an algorithm in MATLAB that ran the thermal CLT calculations for every layup permutation and found the layup with the greatest warpage. Thermal loads were calculated from a temperature difference of $\Delta T = 115^\circ C$, because later we manufactured the composites at an autoclave plateau temperature of 140 °C and carried out the tests at room temperature (25 °C). Fig. 2 illustrates the layup search results, where each blue marker indicates the thermal warpage of one of the layups in ascending order in terms of warpage. At the very beginning, there are symmetric layups with no warpage at all. All the other layups are

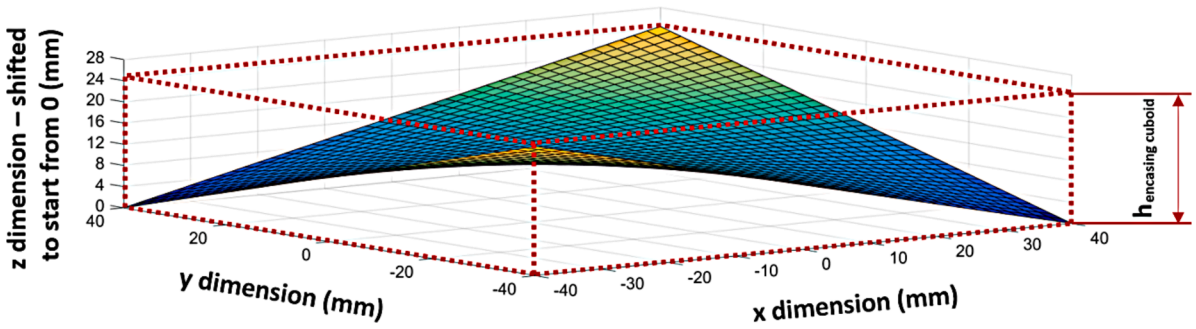


**Fig. 1.** Height of the encasing cuboid ($h_{encasing\ cuboid}$) of a warped laminate.

**Table 1**
Properties of the Hexcel IM7/913 composite material.

| $E_1$(GPa) | $E_2$(GPa) | $G_{12}$(GPa) | $\nu_{12}$ | $t_{ply}$(mm) | $\alpha_0(^\circ C^{-1})$ | $\alpha_{90}(^\circ C^{-1})$ |
|---|---|---|---|---|---|---|
| 163.3 | 8.7 | 4.5 | 0.3 | 0.13 | $3.0 \times 10^{-7}$ | $3.2 \times 10^{-5}$ |

asymmetric and therefore warp when heated or cooled. The laminate with a layup of [45/90/-75/-45] achieved the largest warpage. Therefore, we selected that laminate for the thermally induced mechanical work and warpage mitigation investigations.

## 3. Experimental and numerical methods

First, we experimentally measured the bifurcation point of the chosen layup. The weight-bearing potential of composite laminates was then investigated both numerically and experimentally. From the results, we calculated the thermally induced mechanical work for further evaluation. Furthermore, the warpage mitigation method based on tool compensation was experimentally investigated for both bistable and monostable laminates. Air humidity was a constant 50% during all manufacturing and experimental procedures.

### 3.1. Laminate manufacturing

The composite specimens were manufactured with the autoclave-prepreg technology (Olmar ATC 1100/2000 autoclave and Hexcel IM7/913 prepreg). The prepreg material used comes in 300 mm wide rolls, so the laminate dimensions were chosen to be 210 mm × 210 mm to fit any orientation on the roll width. The laminates were treated in the autoclave at a plateau temperature of 140 °C, while an overpressure of 7 bar was applied. The laminates' uneven edges were then cut, so the final dimensions of the specimens were 190 mm × 190 mm.

### 3.2. Determination of the bifurcation point

To investigate the transition from bistability to monostability, a 12-ply, 190 mm × 190 mm [$45_3/90_3/-75_3/-45_3$] laminate was manufactured on a flat tool. The thicker laminate allowed us to reach lower edge length to thickness ratios during the experiments. The shape of the laminate was 3D scanned with a GOM ATOS Core 5 M scanner at room temperature (25 °C). The scanned points of the surface were imported into MATLAB to fit a second-degree polynomial equation with two variables ($z = ax^2 + bxy + cy^2$), which approximated the warped surface of the laminate well. Then, the principal curvatures were calculated at the mid-point of the laminate. The scanning and the MATLAB evaluation were repeated each time we cut off 5 mm from each edge of the laminate.

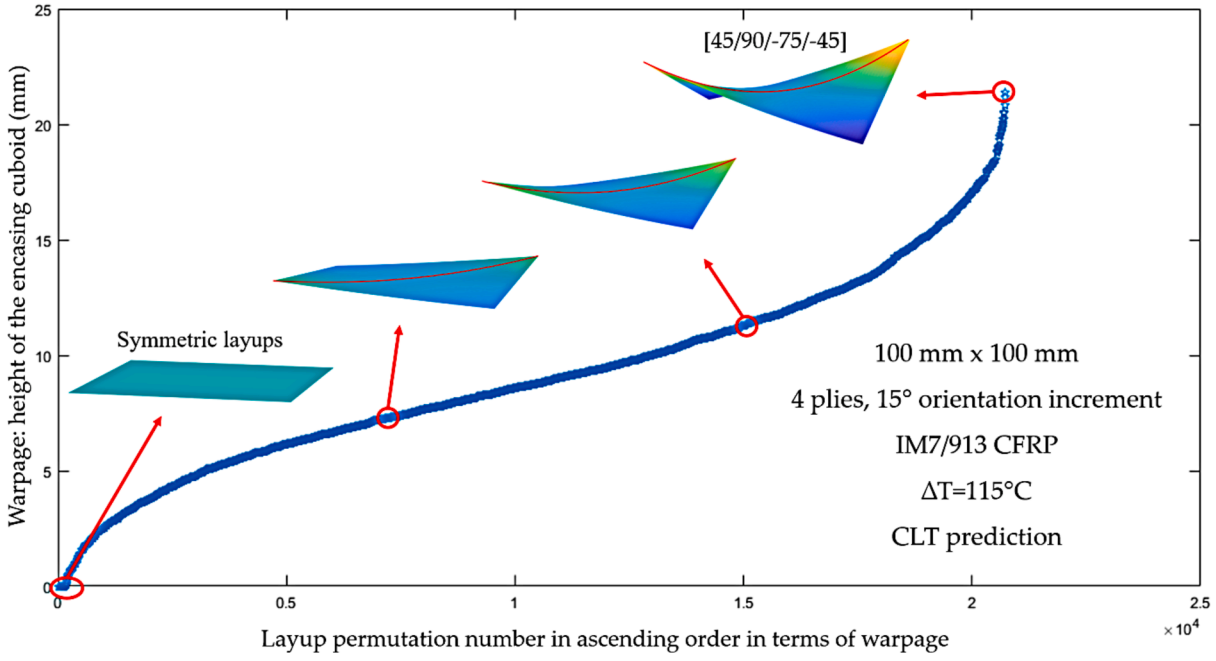


**Fig. 2.** Thermo-twisting layup search based on CLT calculations (4 plies, 15° orientation increment,$\Delta T = 115^\circ C$).

### 3.3. Determination of the thermally induced mechanical work - simulations and experiments

The thermally induced mechanical work of the laminates was calculated from the output data of both numerical simulations and experiments (Fig. 3). The steel tool grabbed a 20 mm × 20 mm area of the 190 mm × 190 mm laminate in the middle of one of its edges. This fixed constraint was chosen to provide adequate support for the laminate without significantly restraining morphing behaviour. Fig. 3/b illustrates the deformation of the laminate after the thermal load. For the experiments, the thermal load was provided by the cool-down from the autoclave's plateau temperature to room temperature, so the laminates were already warped before we placed them into the steel tool. The $h_0$ parameter in Fig. 3/b denotes the maximum vertical deflection of the laminate's corner before the application of the mechanical load. We applied the mechanical load in Fig. 3/c using a Zwick Z005 universal mechanical testing machine with a 5 kN load cell. The tests were repeated with a more sensitive 20 N load cell for the thinner laminates, and the results showed a good correlation with the previous data. As illustrated in Fig. 3/c, the mechanical load ($F$) was applied vertically at the corner with the largest initial deflection. For reliable data, we measured the deflection of the loaded corner ($h_F$) as a function of the applied load ($F$) with a Sobriety Mercury Monet DIC video extensometer. The applied mechanical load was a continuous variable ranging from $F = 0$ N up to the point where snap-through was observed in the case of bistable laminates and where the loaded corner reached the lift height of $h_F = 0$ mm in the case of monostable laminates.

The numerical simulations were carried out with the 2019R3 version of ANSYS. We used 1 mm SOLID185 elements to ensure mesh convergence. A fixed support was applied at the previously mentioned 20 mm × 20 mm area on both sides of the flat laminate. With "large deflections" enabled, the first step of the simulation gave a solution for an applied $\Delta T = -115$ °C (to replicate the cool-down step of the manufacturing process from 140 °C to 25 °C). The second step provided a solution for the applied vertical force at the loaded corner at constant temperature (25 °C). The thermally induced mechanical work was calculated as the product of the applied mechanical load ($F$ in Fig. 3/c) and the lift height under loading ($h_F$ in Fig. 3/c).

### 3.4. Warpage mitigation by laminating on tools with curved surfaces

We attempted to manufacture flat laminates from both the monostable and the bistable regions of the asymmetric layup. To obtain the shapes of the tools, we first manufactured the laminates on flat tools to get warped laminates at room temperature (25 °C). Then, we 3D scanned the shapes of the laminates, created a surface (MATLAB) and then a 3D object (Autodesk Inventor Pro) from the data points, and finally, CNC milled (Roland MDX-540) the tools from aluminium. Then we repeated the manufacturing process, now laminating on the curved tools and flipping the laminates to ensure that deformations occur in the right directions. Flipping was equivalent to laminating $[-45_n/-15_n/0_n/45_n]$ laminates instead of $[45_n/90_n/-75_n/-45_n]$ laminates in the same orientation. After manufacturing, we 3D scanned the shapes of the laminates compensated by the tool and evaluated their warpage in MATLAB. Warpage mitigation based on the tool compensation method enables us to alter the shape of laminates with asymmetric layups at room temperature (or at another selected temperature), while preserving their ability to demonstrate thermally induced mechanical work.

## 4. Results and discussion

In this section, we discuss the results of the experiments and simulations, starting with the determination of the bifurcation point of the $[45_n/90_n/-75_n/-45_n]$ laminate. Next, the thermally induced mechanical work and the warpage mitigation results are evaluated for both monostable and bistable laminates.

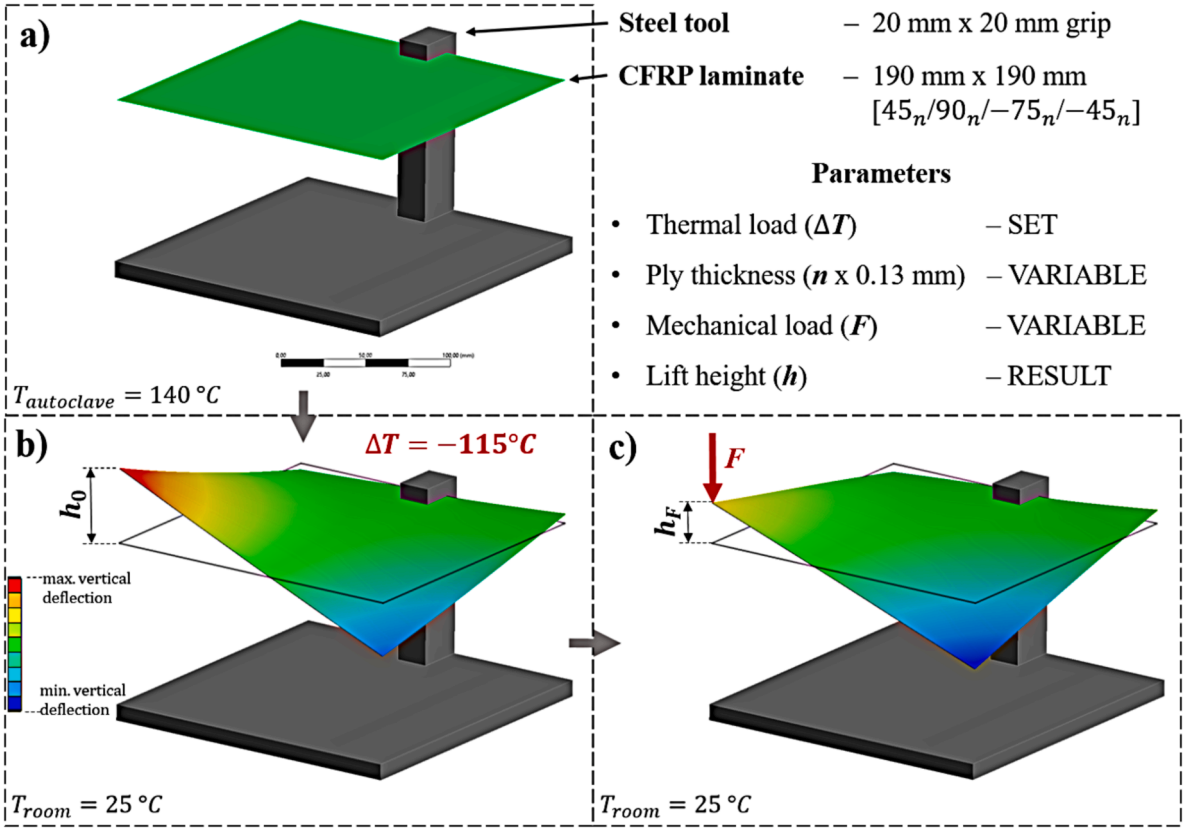


**Fig. 3.** Schematics of the thermally induced mechanical work test setup.

### 4.1. Monostable-bistable transition

Fig. 4 illustrates the experimental results of the determination of the bifurcation point. The results show a characteristic change of the principal curvatures as a function of the edge length to thickness ratio. Based on results in the scientific literature (e.g. [15,16]), the bifurcation point can be identified just below a length to thickness ratio of 60. In Fig. 4, the transition from monostability to bistability is indicated by a local minimum of the first principal curvature and a significant change in the gradient of the second principal curvature. At lower dimensional ratios, there is one stable shape of the laminate, and at higher ratios, there are two. Even in the bistable region, we only investigated one of the stable shapes as it provided all the necessary data for the following experiments and simulations. The results in Fig. 4 agreed well with our observations when we tested the snap-through effect of the laminates. In the bistable region, the second principal curvature converges to zero and the first principal curvature converges to a constant value. With decreasing dimensional ratios, the curvatures start to converge in the monostable region, too.

Based on the results in Fig. 4, we selected a clearly monostable and a clearly bistable laminate for the warpage mitigation experiments. At a dimensional ratio of around 26, we chose a 12-ply [$45_3$/$90_3$/$-75_3$/$-45_3$] 40 mm × 40 mm laminate to represent the monostable behaviour. Similarly, we chose a 4-ply [45/90/-75/-45] 80 mm × 80 mm laminate at a dimensional ratio of around 154 to represent the bistable behaviour. The reason for choosing laminates so far from the bifurcation point was to avoid any transitional behaviour (e.g. a significant second principal curvature of the bistable laminate).

### 4.2. Thermally induced mechanical work

Fig. 5 illustrates the numerically and experimentally obtained deflections of the investigated 190 mm × 190 mm laminates as a function of the applied mechanical load and the number of plies in the specimens. Experiments were carried out up to 28 plies. The experimentally investigated laminates covered the region from monostability (28-ply laminate: a length to thickness ratio of 52) to bistability with negligible second principal curvature (4-ply laminate: a length to thickness ratio of 365). As the transition between bistability and monostability is the most interesting region in terms of the changes in mechanical work, further monostable laminates thicker than 28 plies were not tested to limit prepreg expenditure. Numerical simulations were carried out up to 40 plies providing data deeper into the monostable region. Numerical and experimental results showed a good correlation. Fig. 5 shows that the loaded corners of thinner laminates could not reach the initial flat plane (zero lift height). This was due to the snap-through effect of the bistable laminates. Results are visualised up to the snap-through effect (in case of thinner laminates) or up to the point where the loaded corner reached the initial flat plane (in case of thicker laminates). With increasing thickness, the maximum weight-bearing capacity increased while the maximum deflection decreased. Increasing the number of plies from 4 to 28 decreased the maximum deflection from 117 mm to just 16.5 mm (7 times difference) but increased the maximum weight-bearing capacity from 1.9 N to 65 N (34 times difference).

Fig. 6 illustrates the mechanical work results calculated from the numerical and experimental results in Fig. 5.

The test and simulation results agreed well up to 16 plies and then slightly separated from each other before getting closer together again at 28 plies. The separation took place close to the bifurcation point, where the numerical simulations slightly underestimated the measured mechanical work. Nevertheless, the numerical and experimental results showed a similar trend in terms of thermally induced work.

Fig. 7/a illustrates the change in the maximum achievable work for each laminate as a function of their length to thickness ratio, and Fig. 7/b shows the measured and simulated principal curvatures of the 190 mm × 190 mm laminates as a function of their length to thickness ratio. The two subfigures allow for a visual comparison between characteristic points in the work graph and the stability (principal curvature) graph.

In Fig. 7, we evaluate the results from right to left, starting from the thin bistable laminates and moving towards the thick monostable laminates. The most notable result is that the maximum work goes through a local maximum and then a local minimum. The local maximum of the

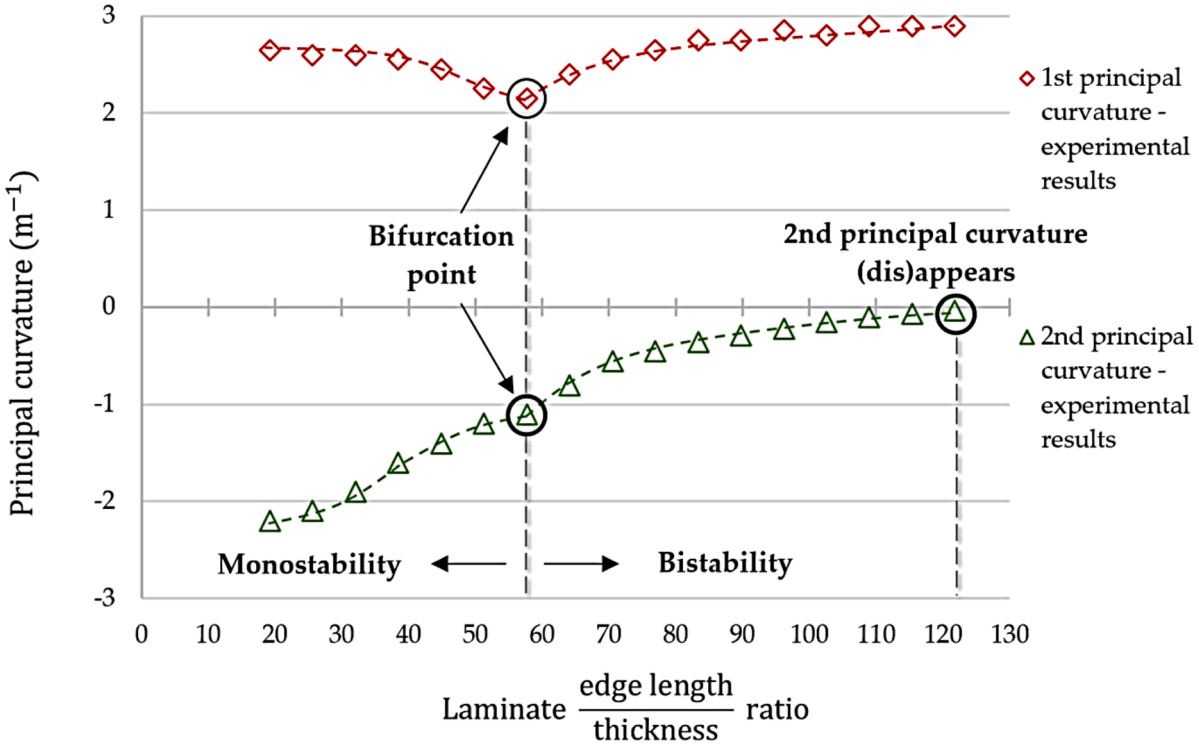


**Fig. 4.** Monostable-bistable transition of the [$45_3$/$90_3$/$-75_3$/$-45_3$] laminate (constant 12-ply laminate).

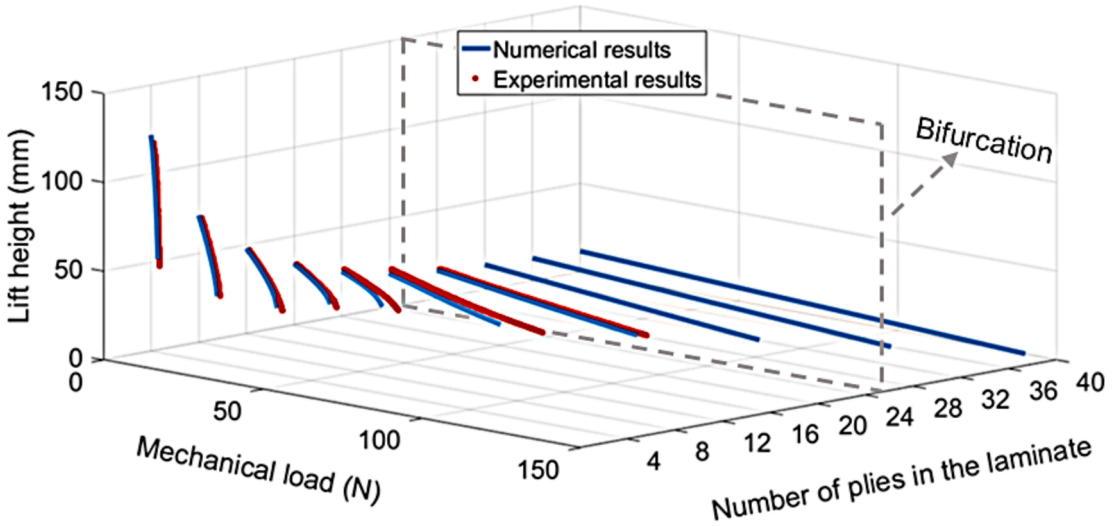


**Fig. 5.** Lift height of the loaded corner of the 190 mm × 190 mm [$45_n/90_n/\text{-}75_n/\text{-}45_n$] laminates as a function of the mechanical load and the number of plies in the laminates - numerical and experimental results. Test setup: Fig. 3, bifurcation: Fig. 4.

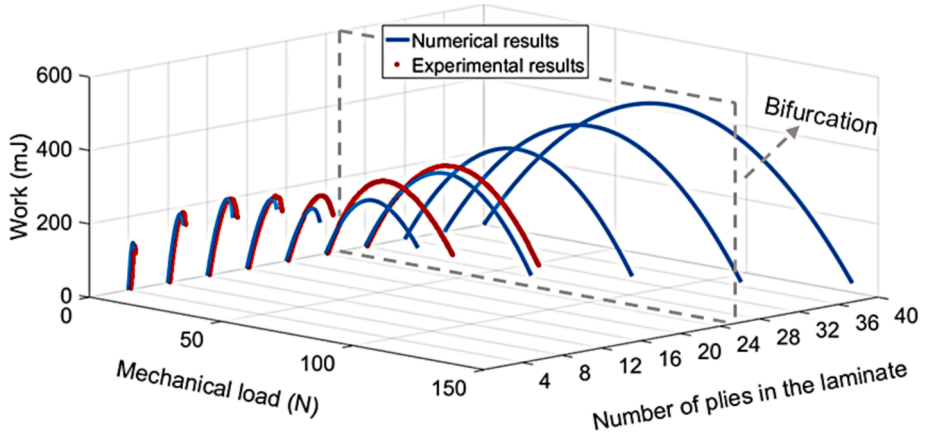


**Fig. 6.** Mechanical work of the loaded corner of the 190 mm × 190 mm [$45_n/90_n/\text{-}75_n/\text{-}45_n$] laminates as a function of the mechanical load and the number of plies in the laminates - numerical and experimental results. Test setup: Fig. 3, bifurcation: Fig. 4.

maximal work can be found at around a dimensional ratio of 125 (12-ply laminate) in Fig. 7/a. Up to that point, the maximal work increases with increasing laminate thickness, which is expected. The local maximum is very close to the appearance of the 2nd principal curvature in Fig. 7/b, implying a causal relationship between the two (i.e. the thermally induced mechanical work decreases because of the appearance and increase of the 2nd principal curvature). Up to that point, the 1st principal curvature decreases, but the 2nd principal curvature is still negligible. However, after the dimensional ratio of 125, the shape of the laminate changes qualitatively, too, with the appearance of the 2nd principal curvature. Note that Fig. 7/b provides similar results to Fig. 4, the main difference being that previously we kept the laminate thickness constant and later, we kept the laminate edge length constant. This resulted in seemingly different graphs, but both the appearance of the 2nd principal curvature (at a dimensional ratio of around 125) and the bifurcation point (at a dimensional ratio of around 60) can be identified in either figure. The local minimum of the maximal work can be found around a dimensional ratio of 70 in Fig. 7/a. The reason why the local minimum of the maximal work does not overlap exactly with the bifurcation point (at a dimensional ratio of around 60) is that the rate of change of the 2nd principal curvature slows down even before the bifurcation point where the effect of the increasing relative thickness (which increases work) outweighs the effect of the increasing 2nd principal curvature (which decreases work).

From a practical standpoint, this characteristic change of the maximal work can be exploited to save weight with bistable laminates. Based on the experimental results, the 12-ply laminates achieved about the same maximum thermally induced work as the laminates twice the thickness, but at larger deformations and lower mechanical loads. The results depend on various factors: e.g. material properties, stacking sequence, laminate dimensions, boundary conditions and load application. The numerical and experimental study in this publication serves as a proof of concept for the influence of laminate stability on the achievable thermally induced mechanical work.

### 4.3. Warpage mitigation

As there are two qualitatively different thermally warped states (monostable and bistable), warpage mitigation needed to be investigated for both cases to draw well-founded conclusions. The ratio of the principal curvatures allows us to sort the shapes into monostable and bistable categories in the investigated range. Based on Fig. 4 and Fig. 7/b, the ratio of the absolute values of the first $\left(\left|\kappa_1^{princ.}\right|\right)$ and the second $\left(\left|\kappa_2^{princ.}\right|\right)$ principal curvatures at the bifurcation point is about 2 (1:0.5). Any ratio significantly higher than this indicates a bistable shape, and a

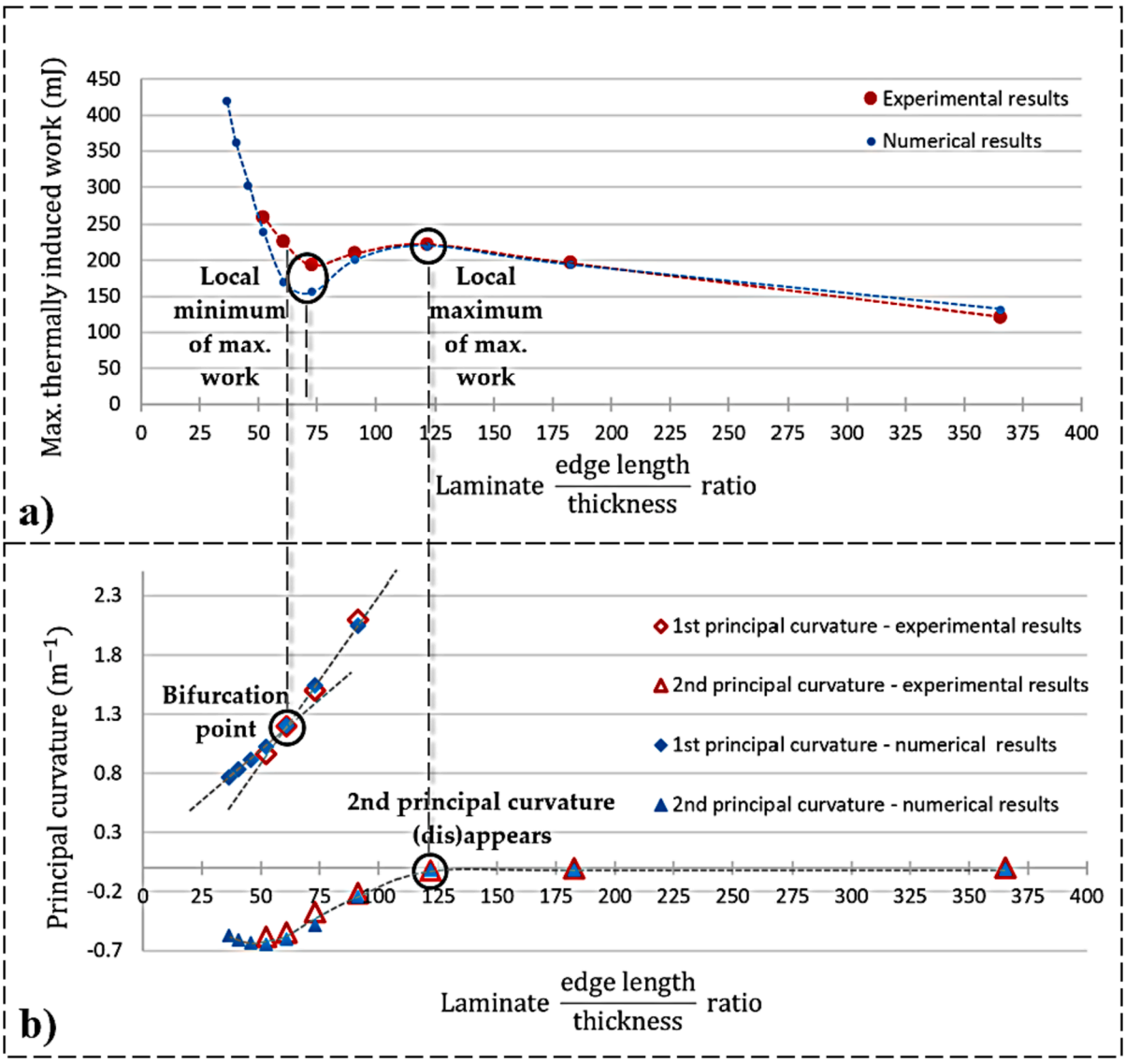


**Fig. 7.** Numerical and experimental results of the a) maximum thermally induced work and b) principal curvatures of the 190 mm × 190 mm [$45_n$/$90_n$/$-75_n$/$-45_n$] laminates as a function of their dimensional ratio (constant 190 mm × 190 mm laminate).

ratio significantly lower than this indicates a monostable shape, as Fig. 4 shows.

Fig. 8 contains all the important data and results for the first warpage mitigation experiment. The top part of the figure illustrates the shape of the aluminium tool on which the composite was laminated before it was manufactured in the autoclave. Section 3.4 discusses the process of tool design. Because the 80 mm × 80 mm [45/90/-75/-45] laminate is bistable when laminated on a flat tool, the curved tool surface only had one significant principal curvature. With the "bistable-shaped" curved tool, we achieved a slight warpage mitigation of 12.4%, shown by the reduction of the height of the encasing cuboid from 12.1 mm to 10.6 mm. The original curvature practically vanished, but the other (so far hiding) principal curvature appeared, resulting in another bistable laminate.

The results suggest that both principal curvatures have to be compensated for at the same time, even if one of them is "hiding" (practically zero) as in the case of bistable laminates. In the next experiment, we designed and manufactured a tool based on the tool in Fig. 8, but now including the second principal curvature with the same magnitude but opposite sign compared to the first principal curvature. This resulted in a "monostable-shaped" tool about twice the height of the tool in Fig. 8. Fig. 9 illustrates the results achieved with the "monostable shaped" tool. Compared to the original bistable laminate, we achieved a warpage mitigation of 23.1%, shown by the reduction of the height of the encasing cuboid from 12.1 mm to 9.3 mm. The warpage mitigation achieved with the "monostable-shaped" tool was almost double what we achieved with the "bistable-shaped" tool. But the most important result is the shape of the final laminate. The manufactured laminate became monostable. This observation was confirmed by the ratio of the principal curvatures, which was 1:0.93.

After successfully transforming the bistable laminate into a monostable one, we investigated the effectiveness of the tool compensation method on monostable laminates. Fig. 10 illustrates the results of laminating the 12-ply [$45_3$/$90_3$/$-75_3$/$-45_3$] 40 mm × 40 mm laminate on a "monostable-shaped" tool. A warpage mitigation of more than 90% was achieved, shown by the reduction of the height of the encasing cuboid from 1.80 mm to 0.17 mm. Furthermore, the final laminate was indistinguishable from a flat laminate; only the 3D scanner revealed the slight residual curvatures. The final laminate satisfied the specification of the ISO2768K standard, and therefore it can be classified as flat.

The results show that the tool compensation method can transform bistable laminates into monostable ones and that it is capable of

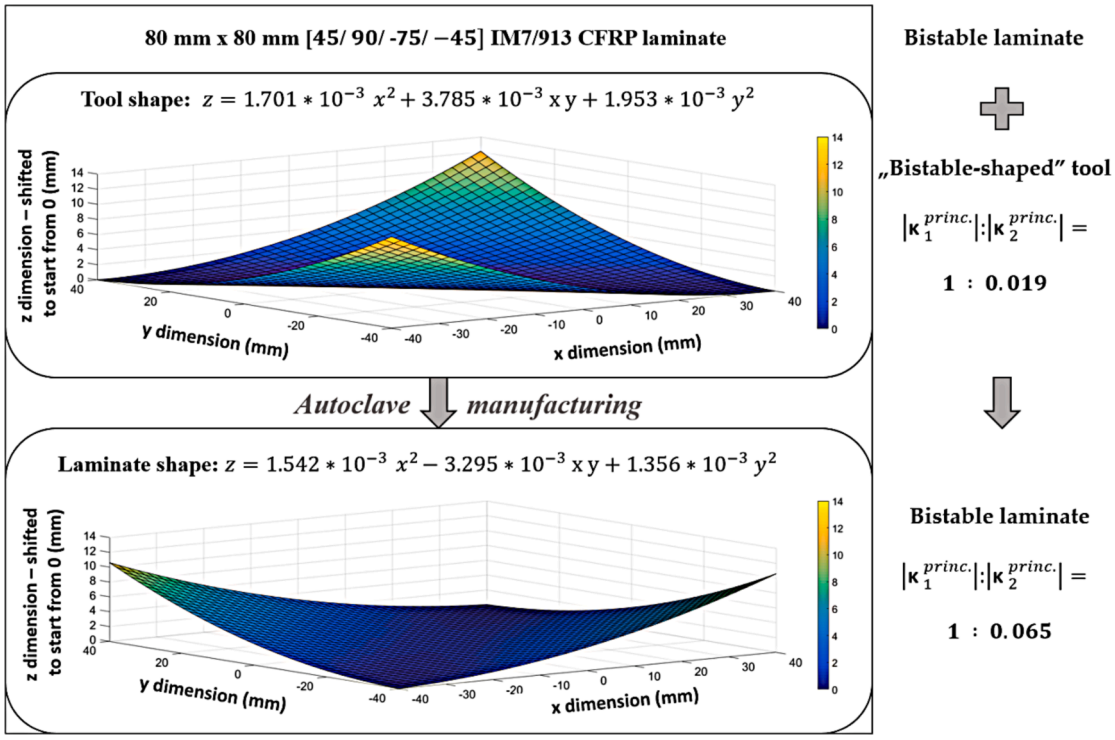


**Fig. 8.** Warpage mitigation results of the 80 mm × 80 mm 4-ply laminate with a single curvature tool.

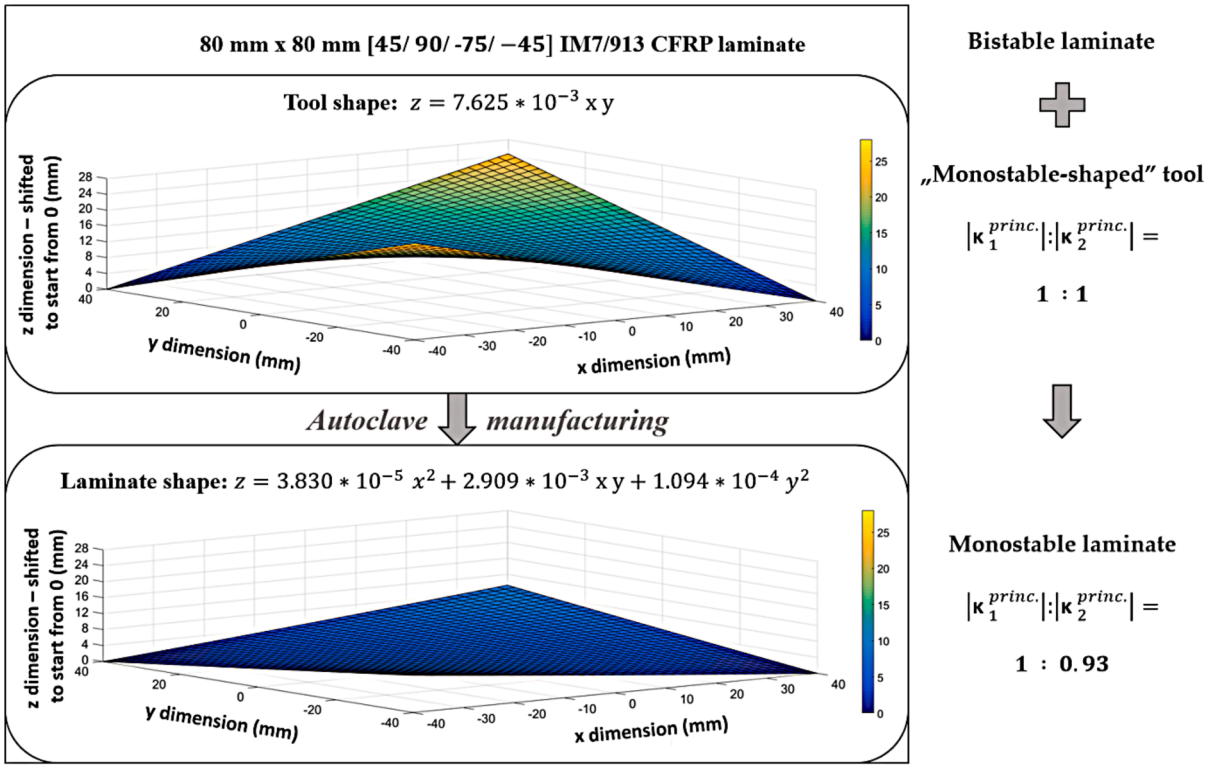


**Fig. 9.** Warpage mitigation results of the 80 mm × 80 mm 4-ply laminate with a double curvature tool.

drastically mitigating the manufacturing-induced thermal warpage of monostable laminates. Based on these findings, we expect that the warpage of bistable laminates can be mitigated with similar success to monostable laminates. The results imply that this requires "monostable-shaped" tools, which we will investigate numerically and experimentally in the future.

## 5. Conclusions

The warpage compensation and the thermally induced mechanical

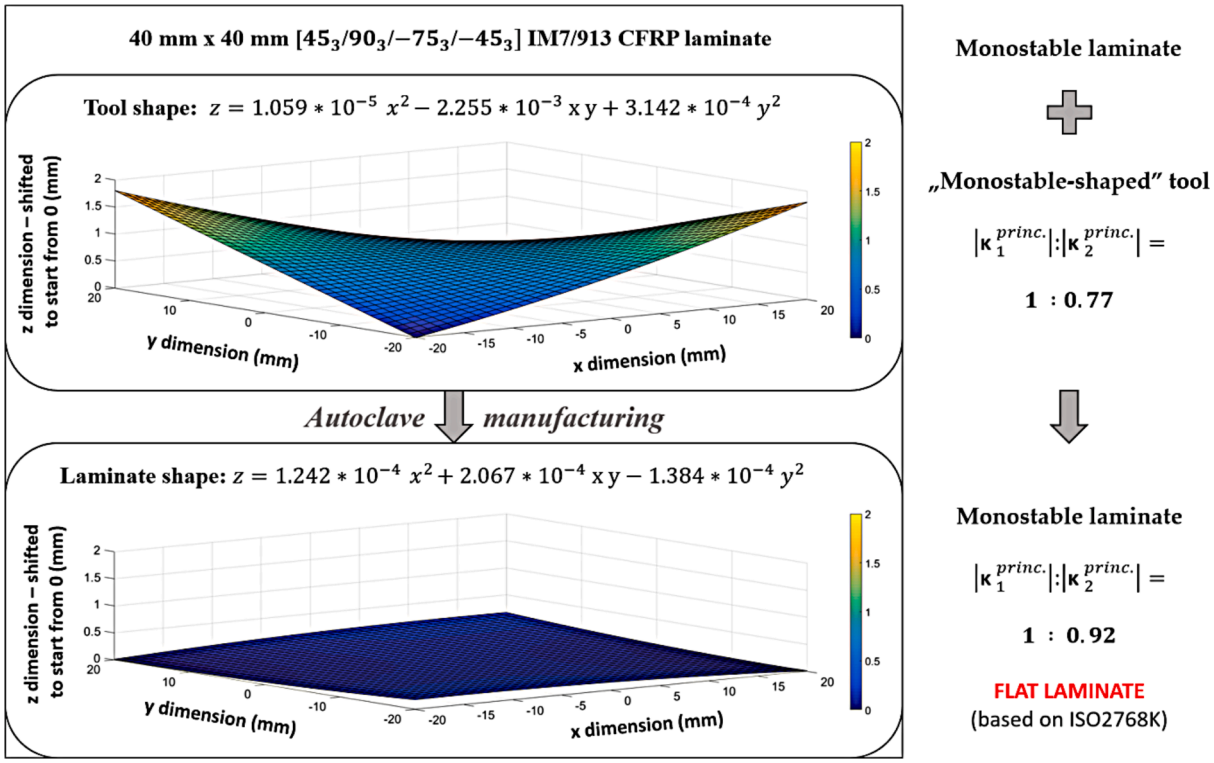


**Fig. 10.** Warpage mitigation results of the 40 mm × 40 mm 12-ply laminate with a double curvature tool.

work of asymmetric laminates are closely related topics. With the warpage compensation method, it is possible to control where the morphed shapes of the laminates will take place in terms of the temperature. For instance, an asymmetric laminate can be manufactured flat at room temperature, so the starting shape for the thermally induced morphing (and therefore the mechanical work) is controllable. This is done without modifying the structure of the laminate, therefore without decreasing its intrinsic morphing performance.

Numerical and experimental results showed that the maximum value of the thermally induced work goes through a local maximum and then a local minimum when the thickness of the laminate is increased (decreasing the edge length to thickness dimensional ratio). The local maximum of the maximal work was associated with the appearance of the second principal curvature of the bistable laminate. Further reducing the dimensional ratio led to a local minimum of the maximal work close to, but just before the bifurcation point. We believe that the effect of the increasing thickness outweighed the effect of the increasing second principal curvature before the bifurcation point, and this is what caused the maximal work values to start increasing before reaching the monostable region. The results presented mean that thinner (and therefore lighter) composites can outperform their thicker counterparts in terms of the maximum achievable thermally induced mechanical work.

The warpage mitigation method based on tool compensation retains the temperature dependence of the shape, which is necessary for exploiting the thermally induced mechanical work of laminates, but it helps to approach the desired laminate shape at a given temperature. Asymmetric laminates from the monostable region (when laminated flat) were successfully manufactured flat (based on the ISO2768K standard) with tools that have both principal curvatures ("monostable-shaped" tools). Furthermore, we successfully transformed laminates from the bistable region into monostable laminates using similar "monostable-shaped" tools. The results imply that manufacturing laminates from the bistable region flat requires tools that include the "hiding" second principal curvature of the laminate.

Safety switches in overheating systems is one of the potential applications of laminates that are capable of thermally induced mechanical work. They work similarly to bimetals, but can perform the same task at a significantly lighter weight which can be critical in aerospace applications, for instance. Another potential application is energy harvesting at locations that experience significant daily temperature fluctuations (e.g. deserts) where energy can be harvested similarly to floating tidal energy harvesting systems in the seas. For these applications, the laminates need further numerical optimization, considering factors such as the 3D geometry of the structure and the expected changes in temperature, and including long-term performance evaluation under cyclic thermal and mechanical loading. Furthermore, although the elastic properties of composites are mainly determined by the reinforcement, the thermally induced changes in the mechanical properties of the matrix should also be considered in the future.

*CRediT authorship contribution statement*

**Bruno Vermes:** Conceptualization, Methodology, Software, Investigation, Data curation, Formal analysis, Validation, Visualization, Funding acquisition, Writing – original draft. **Tibor Czigany:** Conceptualization, Methodology, Funding acquisition, Supervision, Investigation, Validation, Project administration, Resources, Writing – review & editing.

## Declaration of Competing Interest

The authors declare that they have no known competing financial interests or personal relationships that could have appeared to influence the work reported in this paper.

## Acknowledgements

The research reported in this paper has been supported by the NRDI Fund (TKP2020 IES, Grant No. BME-IE-NAT) based on the charter of

bolster issued by the NRDI Office under the auspices of the Ministry for Innovation and Technology. Furthermore, the research was supported by the ÚNKP-20-3 New National Excellence Program of the Ministry of Human Capacities for which Bruno Vermes expresses his gratitude. A special acknowledgement goes to Peter Csvila for his help in manufacturing and testing.

## References

[1] Zhang W, Zheng Q, Ashour A, Han B. Self-healing cement concrete composites for resilient infrastructures: a review. Compos Part B Eng 2020;189:107892. https://doi.org/10.1016/j.compositesb.2020.107892.
[2] Chow WS, Mohd Ishak ZA. Smart polymer nanocomposites: A review. Express Polym Lett 2020;14:416–35. https://doi.org/10.3144/expresspolymlett.2020.35.
[3] Hegedus G, Sarkadi T, Czigany T. Self-sensing composite: Reinforcing fiberglass bundle for damage detection. Compos Part A Appl Sci Manuf 2020;131:105804. https://doi.org/10.1016/j.compositesa.2020.105804.
[4] Forintos N, Czigány T. Reinforcing carbon fibers as sensors: The effect of temperature and humidity. Compos Part A Appl Sci Manuf 2020;131:105819. https://doi.org/10.1016/j.compositesa.2020.105819.
[5] Fuller JD, Wisnom MR. Pseudo-ductility and damage suppression in thin ply CFRP angle-ply laminates. Compos Part A Appl Sci Manuf 2015;69:64–71. https://doi.org/10.1016/j.compositesa.2014.11.004.
[6] Jalalvand M, Fotouhi M, Wisnom MR. Orientation-dispersed pseudo-ductile hybrid composite laminates – a new lay-up concept to avoid free-edge delamination. Compos Sci Technol 2017;153:232–40. https://doi.org/10.1016/j.compscitech.2017.10.011.
[7] Sapozhnikov SB, Swolfs Y, Lomov SV. Pseudo-ductile unidirectional high modulus/high strength carbon fibre hybrids using conventional ply thickness prepregs. Compos Part B Eng 2020;198:108213. https://doi.org/10.1016/j.compositesb.2020.108213.
[8] Panesar AS, Weaver PM. Optimisation of blended bistable laminates for a morphing flap. Compos Struct 2012;94:3092–105. https://doi.org/10.1016/j.compstruct.2012.05.007.
[9] Chillara VSC, Dapino MJ. Review of morphing laminated composites. Appl Mech Rev 2019;72. 10.1115/1.4044269.
[10] Haynes RA, Armanios EA. New families of hygrothermally stable composite laminates with optimal extension-twist coupling. AIAA J 2010;48(12):2954–61.
[11] York CB. Extension-twist coupled laminates for aero-elastic compliant blade design. 53rd AIAA/ASME/ASCE/AHS/ASC Struct. Struct Dyn Mater Conf, Honolulu 2012.
[12] Herath MT, Natarajan S, Prusty BG, St N. Smoothed finite element and genetic algorithm based optimization for shape adaptive composite marine propellers. Compos Struct 2014;109:189–97. https://doi.org/10.1016/j.compstruct.2013.10.016.
[13] York CB. On bending-twisting coupled laminates. Compos Struct 2017;160:887–900. https://doi.org/10.1016/j.compstruct.2016.10.063.
[14] Shakya P, Sunny MR, Maiti DK. Time domain flutter analysis of bend-twist coupled large composite wind turbine blades: a parametric study. Mech Based Des Struct Mach 2020:1–23. https://doi.org/10.1080/15397734.2020.1824796.
[15] Hyer MW. Calculations of the room-temperature shapes of unsymmetric laminates. J Compos Mater 1981;15:296–310. https://doi.org/10.1177/002199838101500401.
[16] Hyer MW. The room-temperature shapes of four-layer unsymmetric cross-ply laminates. J Compos Mater 1982;16(4):318–40.
[17] Emam SA, Inman DJ. A review on bistable composite laminates for morphing and energy harvesting. Appl Mech Rev 2015;67. https://doi.org/10.1115/1.4032037.
[18] Zhang Z, Li Y, Yu X, Li X, Wu H, Wu H, et al. Bistable morphing composite structures: a review. Thin-Walled Struct 2019;142:74–97.
[19] Chillara VSC, Dapino MJ. Mechanically-prestressed bistable composite laminates with weakly coupled equilibrium shapes. Compos Part B 2017;111:251–60. https://doi.org/10.1016/j.compositesb.2016.12.011.
[20] Daynes S, Diaconu CG, Potter KD, Weaver PM. Bistable prestressed symmetric laminates. J Compos Mater 2009;44:1119–37. https://doi.org/10.1177/0021998309351603.
[21] Lachenal X, Daynes S, Weaver P. Review of morphing concepts and materials for wind turbine blade applications. Wind Energy 2013;16:283–307. https://doi.org/10.1002/we.531.
[22] Daynes S, Nall SJ, Weaver PM, Potter KD, Margaris P, Mellor PH. On a bistable flap for an airfoil. Collect Tech Pap - AIAA/ASME/ASCE/AHS/ASC Struct Struct Dyn Mater Conf 2009:1–11. 10.2514/6.2009-2103.
[23] Tawfik S, Tan X, Ozbay S, Armanios E. Anticlastic stability modeling for cross-ply composites. J Compos Mater 2007;41:1325–38. https://doi.org/10.1177/0021998306068073.
[24] Pirrera A, Avitabile D, Weaver PM. Bistable plates for morphing structures: a refined analytical approach with high-order polynomials. Int J Solids Struct 2010;47:3412–25. https://doi.org/10.1016/j.ijsolstr.2010.08.019.
[25] Dano M-L, Hyer MW. Snap-through of unsymmetric fiber-reinforced composite laminates. Int J Solids Struct 2002;39:175–98. https://doi.org/10.1016/S0020-7683(01)00074-9.
[26] Etches J, Potter K, Weaver P, Bond I. Environmental effects on thermally induced multistability in unsymmetric composite laminates. Compos Part A Appl Sci Manuf 2009;40:1240–7. https://doi.org/10.1016/j.compositesa.2009.05.018.
[27] Mukherjee A, Ali SF, Arockiarajan A. Hybrid bistable composite laminates for structural assemblies: a numerical and experimental study. Compos Struct 2021;260:113467. https://doi.org/10.1016/j.compstruct.2020.113467.
[28] Eckstein E, Pirrera A, Weaver PM. Thermally driven morphing and snap-through behavior of hybrid laminate shells. AIAA J 2016;54:1778–88. https://doi.org/10.2514/1.J054648.
[29] Lee AJ, Moosavian A, Inman DJ. A piezoelectrically generated bistable laminate for morphing. Mater Lett 2017;190:123–6. https://doi.org/10.1016/j.matlet.2017.01.005.
[30] Chillara VSC, Ramanathan AK, Dapino MJ. Self-sensing piezoelectric bistable laminates for morphing structures. Smart Mater Struct 2020;29:85008. https://doi.org/10.1088/1361-665x/ab9060.
[31] Vermes B, Tsai SW, Riccio A, Di Caprio F, Roy S. Application of the Tsai ' s modulus and double-double concepts to the definition of a new affordable design approach for composite laminates. Compos Struct 2021;259:113246.
[32] Tsai SW, Sharma N, Arteiro A, Roy S, Rainsberger B. Composite double-double and grid/skin structures - low weight/low cost design and manufacturing. Stanford: Composites Design Group; 2019.
[33] York CB. Tapered hygro-thermally curvature-stable laminates with non-standard ply orientations. Compos Part A 2013;44:140–8. https://doi.org/10.1016/j.compositesa.2012.08.023.
[34] Cui D, Li DK, Zhou SM. Hygro-thermally curvature-stable free-layer composite laminates with extension-twist coupling. Adv Compos Lett 2018;27. https://doi.org/10.1177/096369351802700303.
[35] Fernlund G, Floyd A, Shewfelt M, Hudek M. Process analysis and tool compensation for a complex composite panel. Am Soc Compos - 22nd Tech Conf Am Soc Compos 2007 - Compos Enabling a New Era Civ Aviat 2007;2:1083–94.
[36] Wang Q, Li T, Yang X, Wang K, Wang B, Ren M. Prediction and compensation of process-induced distortions for L-shaped 3D woven composites. Compos Part A Appl Sci Manuf 2021;141:106211. https://doi.org/10.1016/j.compositesa.2020.106211.
[37] Renze SP, Laananen DH. Reduction of composite panel initial curvature by tool compensation. J Thermoplast Compos Mater 1992;5:287–303. https://doi.org/10.1177/089270579200500402.
[38] Eckstein E, Pirrera A, Weaver PM. Multi-mode morphing using initially curved composite plates. Compos Struct 2014;109:240–5. https://doi.org/10.1016/j.compstruct.2013.11.005.
[39] Ryu J, Kong J-P, Kim S-W, Koh J-S, Cho K-J, Cho M. Curvature tailoring of unsymmetric laminates with an initial curvature. J Compos Mater 2012;47:3163–74. https://doi.org/10.1177/0021998312462915.
[40] Barbero EJ. Introduction to composite materials design. 3rd ed. Boca Raton: Taylor & Francis Group; 2018.